COO-4223-4
PSI TR-128

INVESTIGATION OF CONCEPT OF EFFICIENT SHORT WAVELENGTH LASER

Interim Progress Report
1 April 1977 - 30 April 1978

L. G. Piper, R. H. Krech and R. L. Taylor

May 1978

Prepared for
U. S. Energy Research & Development Administration
under Contract No. ES-77-C-02-4223.A002

PHYSICAL SCIENCES INC.
30 COMMERCE WAY, WOBURN, MASS. 01801

DISCLAIMER

NOTICE

COO-4223-4
PSI TR-128

INVESTIGATION OF CONCEPT OF EFFICIENT SHORT WAVELENGTH LASER

Interim Progress Report

1 April 1977 - 30 April 1978

L. G. Piper, R. H. Krech and R. L. Taylor

May 1978

Prepared for

U. S. Energy Research & Development Administration

under Contract No. ES-77-C-02-4223.A002

Physical Sciences Inc.
30 Commerce Way
Woburn, MA 01801

ABSTRACT

This report summarizes progress during the first year of the subject contract. Under this program PSI is investigating the photolytic decomposition of a class of endoergic molecules--azides. Because these compounds contain substantial chemical energy, they offer a potentially more efficient approach for the production of electronically excited fragments. The goal of the present program was to acquire sufficient data and understanding of certain fundamental processes to permit the critical evaluation of this approach for laser development. An apparatus was built to study the wavelength-selected photolysis of gaseous, covalent azides. The photolysis source is a frequency doubled, tuneable dye laser. Detection of fragment species is accomplished by observation of primary fluorescence, or by laser-induced fluorescence (LIF) using a second tuneable dye laser. The design of the apparatus is discussed in detail in this report. Calculations based upon the photolysis of HN_3 were made to determine approximate densities of fragment species and LIF signals to be expected, and the effects of signal noise, fluorescence quenching and diffusion of species out of the detector field-of-view. The photolysis of HN_3 was studied in the apparatus by observing the product $NH(a\,^1\Delta)$ by LIF as a function of delay time after the photolysis pulse, and by observing the temporal behavior of the fluorescence from $NH_2(\tilde{A}\,^2A_1)$ which is produced in the reaction between $NH(a\,^1\Delta)$ and HN_3 with a rate constant of 1.7×10^{-10} cm^3 $molec^{-1}$ s^{-1}. The $NH_2(\tilde{A}\,^2A_1)$ is removed by the HN_3 by electronic quenching and chemical reaction with a rate constant of 8×10^{-11} cm^3 $molec^{-1}$ s^{-1}. Preliminary observations have been made on the photolysis of ClN_3. This molecule dissociates to form $NCl(b\,^1\Sigma^+)$ which emits at 665 nm.

TABLE OF CONTENTS

LIST OF ILLUSTRATIONS

I. INTRODUCTION

It is generally recognized that a laser device possessing all of the properties required as a driver for a practical fusion reactor does not yet exist. Therefore, a substantial effort is currently underway to find and develop such a laser. Some of the desirable characteristics for a laser-fusion driver are short wavelength (300 nm $\leq \lambda <$ 3000 nm), high overall efficiency ($\geq$ 1%), and scalability to large size ($\geq$ 100 kJ/pulse). The development of a laser with the above characteristics, together with acceptable cost and reliability, is acknowledged to be a difficult task, and a number of different technical approaches are being pursued in parallel. For example, one effort is concerned with the photolytic production of group VI atoms such as O or S in the metastable singlet state.

Under the present contract, PSI is investigating the photolytic decomposition of a class of endoergic molecules--azides. Because these compounds contain substantial chemical energy, they offer a potentially more efficient approach for the production of electronically excited fragments. The goal of this phase of the program was not to demonstrate a laser, but to acquire sufficient data and understanding of certain fundamental processes to permit the critical evaluation of this approach for laser development.

Under a previous ERDA contract[1], we reviewed the literature pertaining to the decomposition of azides and concluded that the production of electronically excited species of potential laser interest may be achieved via essentially two major pathways: (i) the photolytic or thermal decomposition of covalent azides to produce electronically excited singlet nitrenes; or (ii) various chemiluminescent reactions of the azide radical. The major task of the present contract was to investigate the first method of electronic-state production, by focussing upon the wavelength-selected photolysis of gaseous covalent azides.

Electronically excited species may be produced in gaseous azide photolysis either as one of the primary fragments of the dissociation process, or as the product of secondary reactions of the azide with its photolysis fragments.[1] For example, in the photolysis of HN_3, the NH radical is produced in the primary photolysis in the $a\ ^1\Delta$ state.[2-6] This electronically excited NH radical reacts with HN_3 to produce $NH_2(\tilde{A}\ ^2A_1)$ which emits throughout the visible and near infrared giving the so-called α-bands of ammonia.[7] This emission has also been observed in thermal decomposition[8] and spark-initiated explosion of HN_3[9]. In addition, the N_3 radical, which is another possible product of the $NH(a\ ^1\Delta) + HN_3$ reaction may recombine with another N_3 to yield electronically excited nitrogen.[1] This sequence of possible reactions is summarized below.

$$HN_3 + h\nu \longrightarrow NH(a\ ^1\Delta) + N_2 \quad \text{(primary photolysis)} \qquad (1)$$

$$NH(a\ ^1\Delta) + HN_3 \xrightarrow{k_2} NH_2(\tilde{A}\ ^2A_1) + N_3 \qquad (2)$$

$$NH_2(\tilde{A}\ ^2A_1) \xrightarrow{k_3} NH_2(\tilde{X}\ ^2B_1) + h\nu \quad (\alpha\text{-bands of ammonia}) \qquad (3)$$

$$NH_2(\tilde{A}\ ^2A_1) + HN_3 \xrightarrow{k_{4a}} NH_2(\tilde{X}\ ^2B_1) + HN_3 \qquad (4a)$$

$$\xrightarrow{k_{4b}} NH_3 + N_3 \qquad (4b)$$

$$N_3 + N_3 \xrightarrow{k_5} N_2(B\ ^3\pi_g) + 2N_2(X) \qquad (5)$$

$$N_2(B\ ^3\pi_g) \xrightarrow{k_6} N_2(A\ ^3\Sigma_u^+) + h\nu \quad (\text{nitrogen } 1^+ \text{ bands}) \qquad (6)$$

$$N_3 + HN_3 \xrightarrow{k_7} \text{products} \qquad (7)$$

$NH(a\ ^1\Delta)$ is metastable and has never been observed in emission to the ground state, while the $NH_2(\tilde{A}\ ^2A_1)$ emission is rather diffuse, and is so rapidly quenched (see below) that HN_3 does not appear to be an attractive candidate for a laser system. However, the HN_3 system is reasonably well characterized experimentally so that by studying HN_3 photolysis, we can obtain a useful calibration of the sensitivity and versatility of our apparatus.

More interesting from a laser standpoint are the halogen azides. They decompose to give an electronically excited halonitrene which subsequently emits radiation, e.g.,

$$ClN_3 + h\nu \longrightarrow NCl(b\ ^1\Sigma^+) + N_2 \qquad (8)$$

$$NCl(b\ ^1\Sigma^+) \longrightarrow NCl(X\ ^3\Sigma^-) + h\nu \quad \lambda_{oo} = 665\ nm^{10} \qquad (9)$$

The $NCl(b\ ^1\Sigma^+)$ is metastable* and would be expected to be fairly unreactive towards other molecules by analogy with studies of NF[11, 13] and NH.[12, 14-17]

In order to evaluate the potential of products from azide photolysis as potential laser candidates, several technical issues must be addressed as follows: (i) the primary products of the photolysis must be identified as a function of photolysis wavelength, (ii) detailed spectroscopy of the electronically excited fragments, such as energy levels and lifetimes, must be obtained, and (iii) the kinetics of chemical and energy-transfer reactions of selected electronically excited species must be determined. To perform these measurements, a photochemical reactor had to be developed in which the wavelength of the photolysis source could be varied, the detection techniques would provide high sensitivity with good temporal resolution, and reasonably well defined spectral diagnostics would be available. The re-

*We estimate a lifetime of about 10 ms by analogy with the $b\ ^1\Sigma^+$ states of NF and NH for which the lifetimes are 15 ms[11] and 18 ms[12] respectively.

quirement of a wavelength-tuneable photolysis source was met with a tuneable dye laser which provided adequate intensity in the spectral region of interest. Sensitive detection has been achieved either by laser-induced fluorescence (LIF) or by direct observation of photon emission. Good temporal resolution is obtained by pulsing the photolysis source and using a gated detection system to monitor species at varying times after the photolytic pulse, or by observing photon-emission traces on an oscilloscope subsequent to the photolysis. Suitable spectral diagnostics include the use of interference filters, a fast monochromator, and/or tuning the laser used in the LIF studies over the absorption bands of the species to be studied.

II. EXPERIMENTAL DESIGN

A. Apparatus

The apparatus constructed for this experiment is shown schematically in Fig. 1. It consists of a stainless steel photolysis cell to contain the azide, which, in some instances, may be mixed with an inert buffer gas. Experiments are carried out either with a slow flow of gas through the cell, or with a static fill. In flow experiments, the gases are metered into the cell by calibrated flow meters and the concentrations of species calculated from the known flow-rates and the total cell pressure, viz

$$[X_i] = \frac{f_{x_i}}{\sum_j f_{x_j}} \times 3.26 \times 10^{16} \times P_{total} , \qquad (10)$$

where f is the flow rate of subscripted species X_i, P_{total} is the total cell pressure, and the units of $[X_i]$ are particles cm^{-3}. The total cell pressure is measured either with a capacitance manometer (Validyne DP-7 for $1 \text{ torr} \leq P_{total} \leq 400 \text{ torr}$), calibrated with silicon oil and mercury manometers, or a thermocouple gauge which has been calibrated against a pressure transducer using the gas of interest.

The azide is photolyzed by pulses from a doubled dye laser which may operate either in the single-shot mode, or repetitively pulsed at repetition rates of 0.5 - 20 Hz. Excited species produced in the photolysis may be observed directly in emission or they may be probed via laser-induced fluorescence with pulses from a second dye laser which is triggered off the photolysis laser after a precisely controlled delay. Fluorescence is detected by a photomultiplier placed at right angles to the plane defined by the photolysis and probe lasers. The current output from the photomultiplier flows to ground through a load resistor which may be varied between 0.10 and 60 kΩ. In the single-shot mode, the voltage drop across the load resistor

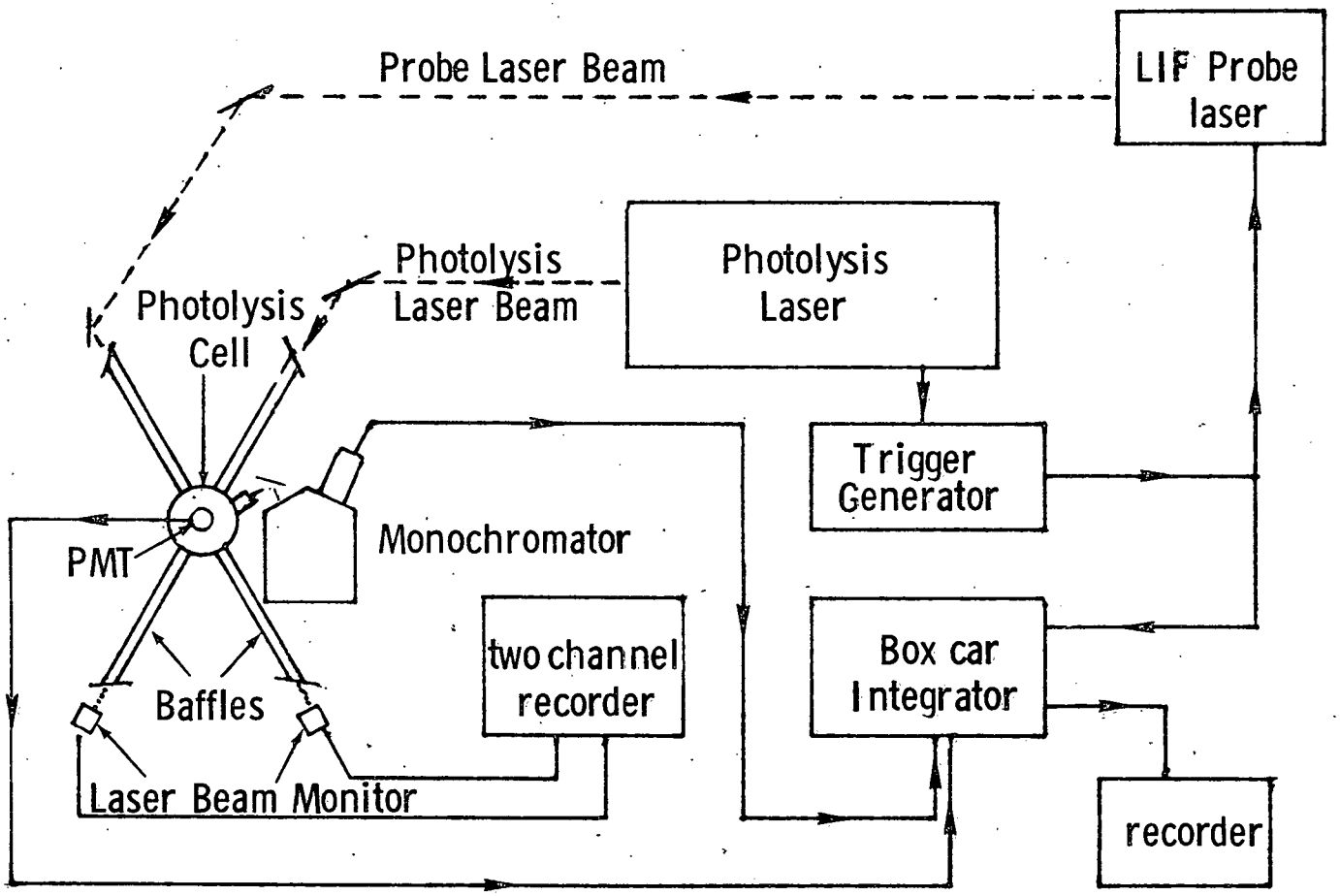

Fig. 1 Schematic of Laser Photolysis Apparatus

is monitored on an oscilloscope which is triggered off the photolysis laser. In the repetitive mode, the signal voltage is fed into a box-car integrator, the gate of which opens as the probe laser is fired. The gate is usually held open for a period of five fluorescence decays of the species of interest so that all fluorescence induced by the probe laser is collected. Interference filters are inserted between the reaction volume and the detector to reject scattered laser light and to provide spectral resolution. In addition, a monochromator can view the photolysis region for cases in which the emission intensities are strong. In repetitive experiments, the average intensities of the two lasers can be monitored so that corrections may be made for long term drift. In the single-shot experiments, a quartz flat in the optical train of the photolysis laser directs about 10% of the laser's output into an energy meter, thus monitoring the laser energy for each shot. As an additional check, the photolysis-laser pulse is monitored with a fast photodiode, and its waveform is displayed on a second trace of the oscilloscope.

The major criterion in choosing the photolysis laser was that it have a high energy per pulse at a moderate pulse-repetition rate. Our choice was the Candela TFDL-1 flashlamp-pumped dye laser which was stated to provide 5 mJ per pulse at 20 pps at 265 nm, more than an order of magnitude better than other lasers available on the market. While the laser did approach specifications, it failed to do so reliably. A number of the problems we had with the operation of this laser were discussed in a quarterly report.[18] Some experiments were done with this laser operating at much reduced energies (~250 μJ). The manufacturer has recently supplied us with a temporary replacement laser of a different design.* This interim laser has provided

*The replacement laser contains a longitudinal-flow dye cell of 3 mm diameter and 34 cm length. The dye is excited by two linear flashlamps of 50J maximum energy loading placed on opposite sides of the dye cell. The output beam is of circular cross section and thus easier to focus into the doubling cell than the rectangular beam of the TFDL-1. This replacement laser yielded a doubling efficiency ~ 2% for a fundamental energy of about 40 mJ.

energies of about 750 μJ at 300 nm (using Rhodamine 6G dye) and has operated with less stability and lifetime problems than the SLL-1. Most of the experiments discussed in this report were done with this second photolysis laser.

In the technique of laser-induced fluorescence, a molecule is excited to a higher electronic state by resonance absorption of radiation from a laser beam. The excited molecules subsequently fluoresce, and a detector is positioned to detect only the induced fluorescence and not laser photons. The intensity of the induced fluorescence is directly proportional to the number of photons absorbed from the laser beam and hence the number density of absorbers. In the following we use the term LIF intensity from species X to mean the fluorescence intensity from the state excited by resonance absorption from species X. This fluorescence intensity will be directly proportional to the number density of species X.

A laser to be used as an LIF probe should ideally have high energy per pulse, short pulse width and precise triggering. However, the high-energy-per-pulse requirement is less important, than the other two requirements. To discriminate against scattered laser light, it is useful to have a short pulse width so that gating on the detection electronics may be delayed until long after the laser pulse has terminated. If the laser-pulse time is comparable to or longer than the fluorescence lifetime of the species being probed, then a significant fraction of the signal of interest will decay before the laser pulse has terminated. The pulse width of a nitrogen-pumped dye laser is about 5 ns, significantly shorter than the lifetimes of most allowed molecular transitions. By contrast, the pulse width of most flash-lamp-pumped dye lasers is on the order of 1 μs. The short pulse width was the major criterion in our selection of the Molectron N_2 pumped dye laser (DL-200) for the LIF technique. Calculations (discussed below) indicated that the energy per pulse of this laser was more than adequate for our applications.

Photoelectric detection may be done either in the analog mode, i. e. measuring a current or voltage drop across a load resistor, or in the photon-counting mode. Our calculations for expected experimental conditions indicated that signal levels would be more than adequate for analog detection, in most instances being sufficiently large to obtain reasonable signal levels for one-shot display of fluorescence on oscilloscope traces, i. e., photon-emission rates greater than ~ 5 photoelectric events per μs.

One of the major problems associated with laser-photolysis experiments and laser-induced fluorescence detection is scattered light excited by the lasers. The radiation arises not only from scattered photons from the laser beam, but also by fluorescence from cell materials which have been excited by photons scattered from the laser beam. This fluorescence can be an especially severe problem because it may be of long duration compared to the laser pulse, and cannot readily be avoided by delaying the opening of the box-car gate. The experimental cell has been designed to reduce as much as possible interference from scattered laser light and fluorescence from cell materials. This reduction has been achieved by paying careful attention to the laser-delivery system, to the fluorescence-detection system, and by constructing the reaction cell out of chemically blackened stainless steel rather than glass. This latter precaution reduces significantly fluorescence from cell materials. While scattered light was not always completely eliminated, it was not a significant problem in most experiments.

The laser-delivery system involves both the proper introduction of the laser beams into the cell and the proper focussing of these beams inside the cell. The laser beams enter and exit the cell through 55 cm long side arms. Inside each side arm are two conical light baffles, the apexes of which point toward the Brewster's angle entrance and exit windows. The baffles have a cone angle of 60° and have 1/4 inch diameter holes bored through their centers. The main purpose of the baffles is to reduce forward scattering off the entrance and exit windows. They do not significantly skim

the edges of the laser beam as this skimming is more likely to enhance scattered light rather than reduce it. Proper focussing of the laser beams is more useful in reducing stray photons coming from the beam's edges.

The Molectron beam is focussed into the cell by a 100 cm f. l. quartz lens placed approximately 135 cm from the laser 375 cm from the center of the cell. This lens images the focal spot of the laser beam in the doubling crystal at the center of the cell with a magnification of about 3. The spot size at the center of the cell is less than 1 mm in diameter, while the spot at the entrance and exit windows is less than 2 mm. With this arrangement, scattered light from the Molectron has been minimal.

The Candela laser with its much greater pulse energies requires a more stringent focussing to eliminate scattered light. The beam is focussed into the center of the cell with a Kepplerian telescope arrangement with a pinhole at the focus of the two telescope elements. The output lens of the telescope images the pinhole in the center of the cell with a magnification of about 10. This imaging of the pin hole essentially eliminates the edges of the laser beam. The edges of the unfiltered beam would be intercepted by the light baffles in the side arms and would add to scattering problems. The size of the Candela-laser beam at its focus in the center of the cell is about 4 mm. This focussing system, when coupled with the selective detection system, significantly reduced scattered light from the Candela laser.

The optical detection system combines efficient light collection with good stray-light rejection afforded by spatial filtering and the use of interference filters. Light from the interaction region is collected with a 50 mm dia, f/1 lens placed 50 mm from the interaction region. The parallel light rays exiting from the collection lens are refocussed upon the photocathode of the photomultiplier with a 50 mm dia, f/1. 5 lens placed immediately behind the collection lens. This system magnifies the image in the observation region about 1. 4 times, thus giving a 31 mm diameter field-of-view in the cell when viewed with a 44 mm diameter photocathode. The f-number

for light collection of this system is about 1.25, giving a light collection efficiency of 4%. The collection system is very effective in reducing scattered light, since only a very restricted region of space within the photolysis cell is accessible to the detector. Further discrimination against scattered light is provided by the use of interference filters placed between the collection lenses and the photomultiplier. The disadvantage of this light collection system is that the restricted field-of-view resulting from the spatial imaging can degrade temporal information. At low pressures, the time required for a molecule to diffuse from the detector field-of-view can become short compared to molecular-fluorescence life times or to chemical reaction times. Diffusion may be slowed by using an inert buffer gas at high pressure, if quenching of the fluorescence by the buffer gas is not too significant. This is true for most diatomic molecules even at pressures of a few hundred torr; however, for polyatomic molecules such as $NH_2(\tilde{A}^2A_1)$,[19] quenching by the bath gas is significant, so that operation at low pressures and with a larger field-of-view is necessary.

B. Supporting Calculations

Calculations were performed using the photolysis of HN_3 as an example to test the feasibility of the experiment. The HN_3 system has been studied in sufficient detail that reasonably accurate calculations are possible. These results give an indication of the sensitivity and flexibility of the apparatus. In addition, the initial photolysis experiments were performed on HN_3, and these data compared against the calculations provide a final test of apparatus performance.

McDonald et al.[2] have claimed that photolysis of HN_3 at 266 nm produces $NH(a^1\Delta)$ and $N_2(X^3\Sigma_g^+)$ in over 99% yield. The $NH(a^1\Delta)$ appears to be highly reactive toward HN_3 producing $NH_2(^2A_1)$ and presumably N_3. McDonald et al. have not attempted to observe N_3 in their system, but others report it as being present as a secondary product of the photolysis.[3-6]

The experiments of McDonald et al. do not preclude the possibility that N_3 may also be formed in the primary photolysis as others have suggested,[4-6] nor do they indicate the origin of other states of NH which have been observed by others in photolytic systems.

In the following sections we reproduce the calculations performed to test the experimental concept. First, we compute the density of fragments produced in the photolysis laser beam and the signal level to be expected by probing this fragment density with LIF both in terms of photon flux incident upon the PMT photocathode and the voltages to be measured by the boxcar integrator. In the latter computation we also treat sources of signal noise. Finally, we consider the effects of fluorescence quenching and diffusion upon the expected signals.

1. Density of Photolysis Products - The density of photolytic fragments produced by absorption from the photolysis laser pulse may be calculated using Beer's Law,

$$\frac{N}{V} = \frac{I_o - I}{A\ell} = \frac{I_o}{A\ell}\left(1 - e^{-C\sigma_\lambda \ell}\right) \quad , \tag{11}$$

which in the thin target limit reduces to

$$\frac{N}{V} \approx \frac{C\sigma_\lambda}{A} I_o \quad . \tag{12}$$

N/V is the fragment density produced by a laser beam of initial intensity I_o and cross sectional area A propagating a distance ℓ through HN_3 at concentration C. The absorption cross section at wavelength λ is given by σ_λ. I is the intensity of the laser beam after it exits the cell. For a typical condition of our experiment, the following values are appropriate:

$$C = 10^{14} \text{ molec cm}^{-3},$$
$$\sigma_{285} = 5.15 \times 10^{-20} \text{ cm}^2,^{20}$$
$$A = 0.126 \text{ cm}^2 \text{ (4 mm dia spot size)}$$
$$I_o = 0.50 \text{ mJ} = 7.17 \times 10^{14} \text{ photons.}$$

This leads to a transient fragment density,

$$\frac{N}{V} = 2.93 \times 10^{10} \text{ molec cm}^{-3} ,$$

This is the density of $NH(a^1\Delta)$ produced in the photolysis before losses due to chemical reaction and/or diffusion have occurred.

2. LIF Intensity - The $NH(a^1\Delta)$ is detected by LIF operating upon the $c^1\pi \rightarrow a^1\Delta$ transition at 326 nm. The calculation of the signal due to LIF assumes no quenching of the $NH(c^1\pi)$ fluorescence. The optical system is designed to have an effective f-number of 1.25 corresponding to collection of 4% of the total fluorescence. We also assume the photomultiplier quantum efficiency, η, is 0.33 and the transmission of the optical system, T, the product of the transmission of the collection lenses (0.80) and interference filter (0.20), is 0.16. The probe laser intersects the observation region at right angles to the photolysis laser, thus giving an effective absorption path length for the probe laser of 0.4 cm. The fluorescence signal at the detector is then the number of photons absorbed from the probe-laser beam by NH multiplied by the collection efficiency of the optical system, the quantum efficiency of the photomultiplier, and the transmission of the lenses and filters in the optical system:

$$I_f = (I_o - I) \frac{\Omega}{4\pi} \eta T. \qquad (13)$$

The absorption of photons in the probe laser beam by the photolysis fragments can be calculated adequately by line-absorption formulae. The details of the

calculation have been given previously.[22] The line width of the absorbers was assumed to be Doppler at 300°K, while the line-width of the probe laser, measured by scanning the laser over several absorption lines of OH and $NH(a^1\Delta)$, was ~ 0.02 nm FWHM at 300 - 330 nm. The calculation assumed that the absorption was on the P(2) transition for which the absorption oscillator strength is 2.17×10^{-3}.[22] Twenty-five percent of the total $NH(a^1\Delta)$ population will be in $J'' = 2$ at 300°K. Given a probe-laser energy of 0.5 μJ and a total $NH(a^1\Delta)$ density of 2.9×10^{10} molec cm^{-3} as calculated above from Eq. (12), we calculate a fluorescence intensity of 3.8×10^3 photoelectric events per laser pulse.

This calculation assumes perfect alignment of the two lasers which is difficult to achieve in practice. Even very small misalignments, or beam wander of as little as a mrad can lead to large changes in signal level. Still, the large magnitude of the calculated signal indicates a detection sensitivity on the order of 10^7 molec cm^{-3} ought to be achievable.

3. PMT Signal and Noise - The output from the photomultiplier is a current pulse, which is shunted to ground through a load resistor, R_L, producing a voltage detected by the box-car integrator. The value of R_L is made as large as possible to maximize the voltage within limitations imposed by the box-car gate width and the capacitance of the line between the PMT and the input of the box-car. Optimum values of the PMT $R_L C_L$ time constant are between 0.02 and 0.2 times the box-car gate width,[23] e.g., for τ_{gate} = 2.0 μs, the time constant = 40-400 ns. In order to minimize C_L, the cable length between the PMT and the box-car must be kept short. It is easiest to do this if a preamplifier is inserted close to the PMT output. Then, cable lengths of a few feet are feasible for which $C_L \sim 100$ pf and R_L will be $\sim 10^3 \Omega$.

The voltage signal read by the box-car is

$$V_s = \frac{\eta N G e R_L}{\tau_{gate}} \quad . \qquad (14)$$

η is the PMT quantum efficiency, N is the number of photons incident upon the photocathode, G is the PMT gain and e is the electron charge. For a typical gain of 10^6, $R_L \sim 10^3 \Omega$ and $\tau_{gate} = 2\ \mu s$, the voltage will be 80 μV per photoelectric event (ηN), or 80 mV for 10^3 photoelectric events per laser shot.

Sources of signal noise[24] are statistical fluctuations in the signal source, dark noise generated within the PMT, thermal noise in the load resistor, and amplifier noise in the box-car preamplifier. Calculations performed previously[22] indicate that the only significant source of noise will be statistical fluctuations in the signal source. This noise can be reduced an arbitrary amount by signal averaging.

4. LIF Fluorescence Quenching - The reduction of the fluorescence signal by collisional quenching may be calculated from the Stern-Volmer relationship[21]

$$\frac{I}{I_o} = \frac{1}{1 + \tau_{rad} k_q [Q]} \quad . \tag{15}$$

For $NH(c\,^1\pi)$, $\tau_{rad} = 4 \times 10^{-7}$ s.[25] If we assume a quenching rate constant of 1×10^{-10} cm^3 molec^{-1} s^{-1}, then the reduction of fluorescence is less than 10% for quencher concentrations less than 2.5×10^{15} molec cm^{-3} or about 100 mtorr. This is not a severe limitation except for the inert buffer gas which will be at higher pressures. However, rate constants for quenching of electronic energy by gases such as helium and argon are generally $\leq 1\text{-}5 \times 10^{-16}$ cm^3 molec^{-1} s^{-1}. Thus, buffer-gas pressures of several hundred torr should not significantly reduce fluorescence due to collisional quenching. For kinetic experiments in which the LIF intensity is measured as a function of delay time between the photolysis and probe lasers, quenching of the fluorescence will be the same at all delay times, and therefore will not affect the kinetic measurements.

5. Diffusion - The problem created by diffusion is that the species of interest could diffuse out of the detector field of view prior to being observed, i.e. prior to fluorescing if the species emits radiation, or prior to being probed via the LIF laser for those species detected by LIF. In general, when the species of interest are lost not only by diffusion, but also by some first-order, or pseudo first-order process such as fluorescence or chemical reaction, the problem of losses by diffusion may be uncoupled from the other losses resulting in an expression of the form[26]

$$\frac{[C]}{[C]_o} = e^{-t/\tau f_{diff}} \quad . \tag{16}$$

τ is the first-order decay time, i.e. τ_{rad} for radiation or $(k[Q])^{-1}$) for a bimolecular reaction under pseudo first-order conditions ($[Q] \gg [C]$), $[C]$ is the concentration of the species of interest, $[C]_o$ its concentration at $t = 0$, and f_{diff} represents the functional form of the diffusion term which depends upon the diffusion coefficient, D, the time, and the geometry of the viewing region. This latter function may be quite complex. For the case at hand, for which the radius of the viewing region is about 1.5 cm and the laser beam diameter is about 4 mm, the diffusion term near $t = 0$ can be approximated by[26b]

$$f_{diff} \approx (1 - 0.50\ Dt) \quad . \tag{17}$$

Diffusion will have less than a 10% effect upon the chemistry in the photochemical reactor if $Dt < 0.20$. For a typical diffusion coefficient of 160 cm^2 s^{-1} at 1 torr, diffusion will have little effect upon results if

$$t < 1.25P \quad , \tag{18}$$

for P in mtorr and t in μs. Diffusion was not a problem in the experiments described below because the ratio t/P was usually less than one.

III. EXPERIMENTAL RESULTS

A. LIF Tests on OH

The purpose of these experiments was to gain some experience in measuring radical concentrations via the LIF diagnostic, and to obtain an estimate of the sensitivity of our apparatus.

The OH is produced at a calculable concentration via chemical reaction in a flow system external to the cell. The OH radicals then pass into the cell and are detected via LIF in the wavelength region around 308 nm.

The OH is produced by the well known reaction

$$H + NO_2 \rightarrow OH + NO \quad . \tag{19}$$

The H atoms are produced in a microwave discharge in a flow of helium containing traces of added hydrogen. Provided the H atoms are in excess, the flow of OH produced will be equal to the flow of NO_2 added. In the absence of losses due to diffusion or chemical reaction, the concentration of OH can be calculated from

$$[OH] = \frac{f_{NO_2}}{f_{total}} \times p_{total} \times 3.26 \times 10^{16} \quad , \tag{20}$$

where the f's denote the flows of the subscripted species and p_{total} is the reactor pressure in torr. The concentration is in units of molecules cm^{-3}. Because the mean residence time of gas in the cell is on the order of 100 ms, and, as the recombination coefficients of most free radicals upon metal surfaces are usually large, it is probable that there are some losses between where the OH is formed and where it is detected. For this

reason, the concentrations measured within the observation region are upper limits. Provided the initial concentration of OH is below a few $\times 10^{12}$ molec cm^{-3}, gas-phase recombination of the radicals will be negligible, and all other loss processes will be pseudo first order. Thus, the concentrations determined will be accurate on a relative basis.

The Molectron laser provided about 3 μJ of uv radiation at 308 nm using Rhodamine 610 dye. Transmission and reflection losses within the optical train will reduce the actual laser energy in the observation region to about half this value.

The detection system employed a Corning glass filter (CG-7-51) to eliminate visible fluorescence radiation from cell materials which are excited by scattered photons from the laser beam. The filter has a transmission of about 30% at 308 nm, so that attenuation of the OH fluorescence is not too severe. The presence of the filter and a 12 mm dia mask over the filter, which effectively limits the detector field-of-view to about 20 mm, reduced the scattered laser light plus its associated induced cell-materials fluorescence to negligible levels, provided the cell had been under vacuum for several days. Laser scattering off dust in the air is quite severe in a cell which has been recently vented to the atmosphere.

Very strong fluorescence from OH was observed for a number of lines between 306 and 309 nm. The wavelengths of the fluorescence excitation lines we measured have been positively identified by comparisons with the results of other workers.[27]

The box-car was scanned in time to measure the fluorescence decay resulting from excitation of the $R_2(4)$ line at 307.44 nm. The box-car gate width was 30 ns and the PMT load resistor was 50Ω. The semi-log plot of the decay is shown in Fig. 2. The extracted lifetime from these data for the $v' = 0$, $N' = 5$ level of OH $A^2\Sigma^+$ is 0.72 μs which is in excellent agreement with a value of 0.712 μs obtained by interpolation of German's data.[28]

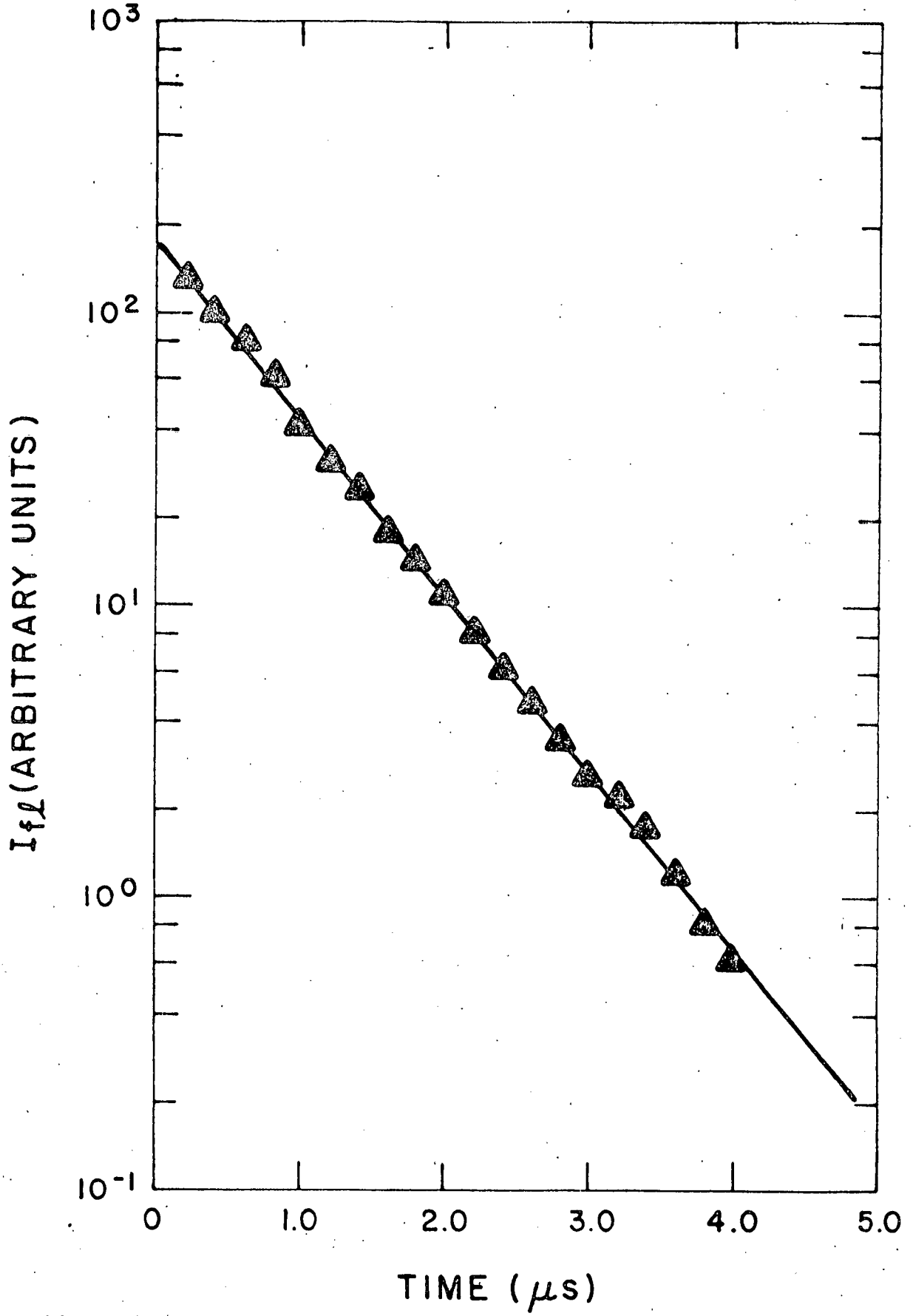

Fig. 2 Fluorescence Decay of OH($A^2\Sigma^+$, $v' = 0$, $N' = 5$). $t_{decay} = 0.72$ μs.

This value subsequently has been confirmed in Kinsey's laboratory.[29] The concentrations of added H, H_2, and NO_2 were less than 0.1 mtorr so that electronic quenching of the OH was negligible.[28]

In order to obtain some estimate of the sensitivity of our apparatus, we tuned the laser to the strong doublet at 308.17 nm which is composed of the $Q_1(3)$ and $P_1(1)$ lines and measured the LIF signal as a function of added NO_2 for a roughly 40-fold excess of H. The results are shown in Fig. 3 where the box-car voltage using a 1.1 kΩ load resistor and 2.0 μs gate width, is plotted against the concentration of OH which would obtain in the absence of any losses due to diffusion or chemical reaction. The box-car signal was about 1 volt for $[OH] \sim 8 \times 10^{10}$ molec cm^{-3}. Given the negligible scattered light conditions obtained under the conditions of the test, a box-car signal of 10 mV would have been well above the noise. Thus, the sensitivity of the apparatus to OH is at least 8×10^8 molec cm^{-3}, and probably somewhat better than this, given that some loss of OH is likely to occur between the region where it is formed and where it has been measured. Considering probable OH losses, that some improvements to the collection system can be made, and that the NH transition probabilities for absorption and emission are greater than those for OH, our estimate of an apparatus sensitivity on the order of 10^7 molec cm^{-3} for NH seems reasonable. Rough calculations based upon experiments on HN_3 discussed in the next section indicate a sensitivity for $NH(a^1\Delta)$ within an order of magnitude of this value.

B. Photolysis of HN_3

Two types of experiments were performed on HN_3. First, the HN_3 was photolyzed and the density of the $NH(a^1\Delta)$ fragments was probed at varying times after the photolysis pulse via LIF. These experiments were done with gas slowly flowing through the cell at total pressures between 5 and 50 torr and HN_3 partial pressures between 0.3 and 20 mtorr. In the other measurements, the cell was filled with pure HN_3 to pressures between 3 mtorr and

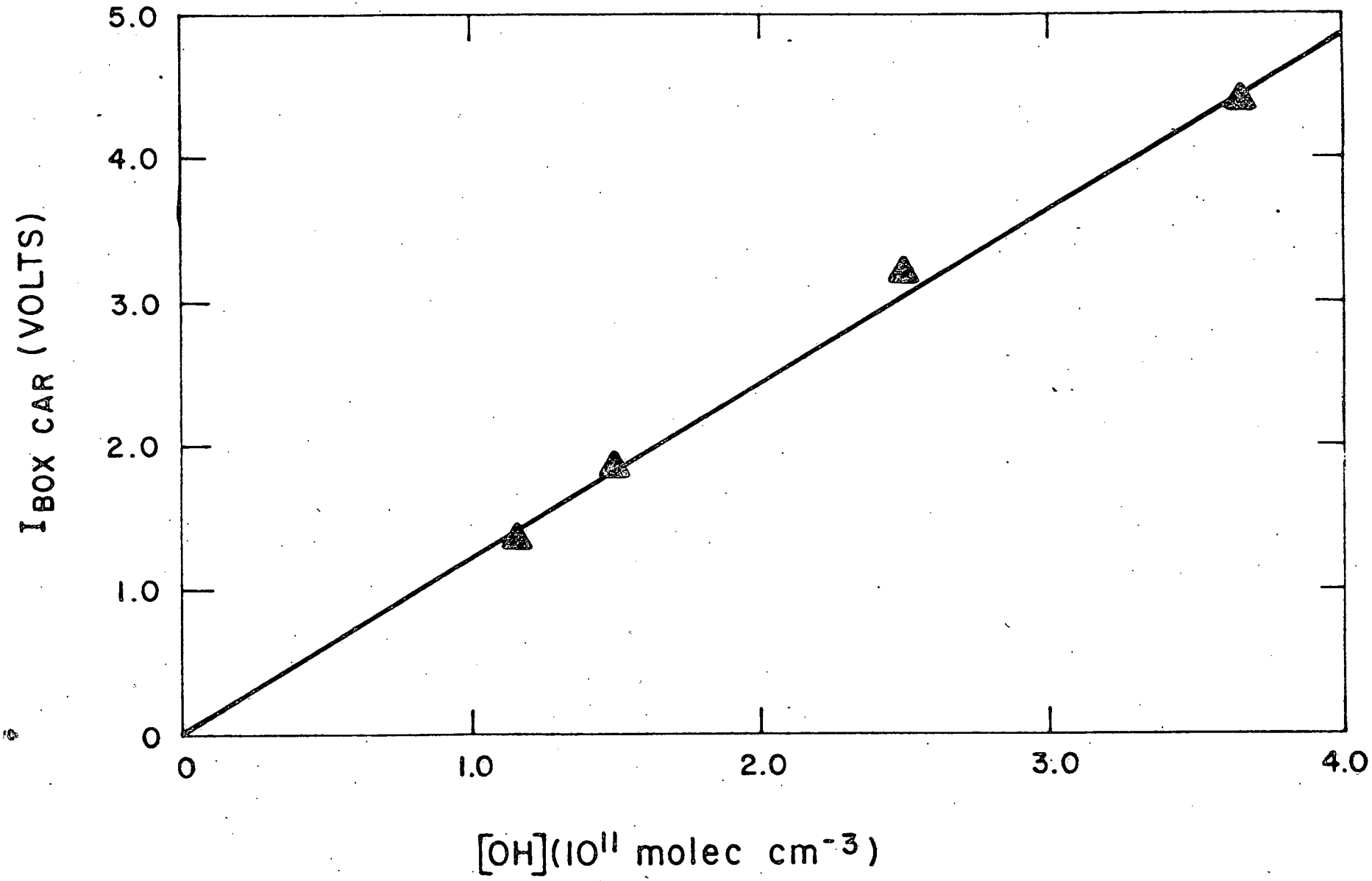

Fig. 3 LIF Intensity of OH as a Function of Added [OH]. The values for [OH] are upper limits. See text for details.

2 torr, and all fluorescence resulting from the photolysis was observed as a function of time after the photolysis-laser pulse. The fluorescence was observed through a Corning, CG 2-62 colored-glass filter (600 nm cutoff, long-pass filter), and with an EMI 9659 QA photomultiplier, giving an effective spectral bandpass of about 600 to 900 nm. In some experiments, fluorescence was observed through an interference filter centered at 454 nm. In these experiments scattered light from the photolysis laser obscured the fluorescence trace at early times; however, the decay rates deduced from 454 nm radiation after termination of the photolysis pulse were the same as the decay rates deduced from the red emission at the same pressure.

In the experiments on the photolysis of HN_3 with the subsequent detection of $NH(a^1\Delta)$ via LIF, the P_2 - P_5 and Q_2 - Q_6 lines of the $NH(a^1\Delta v' = 0 \rightarrow c^1\pi v' = 0)$ transition were positively identified via comparison with published spectra.[30] Figure 4 is a plot of the LIF intensity from the P_2/Q_5 lines at 325.9 nm as a function of $[HN_3]$. The finite intercept was the signal observed in the absence of added HN_3 and results from scattered light from the probe-laser pulse. The data were taken with a photolysis-laser energy of about 125 μJ and a probe laser energy of about 0.5 μJ. Even under these conditions of reduced photolysis energy, it can be seen that a signal well above background is produced at $[HN_3] \sim 10^{13}$ molec cm^{-3}, i.e., at pressures less than a millitorr. The departure from linearity at the higher concentrations may result from removal of the $NH(a^1\Delta)$ by HN_3, either via chemical reaction or electronic quenching during the period between the photolysis pulse and the probe pulse (about 2 μs), and perhaps some degradation in the photolysis laser's output.

Analysis of oscilloscope traces of the $NH(c^1\pi, v' = 0)$ fluorescence decay indicates a lifetime of about 0.47 μs, within the range of reported values which are between 0.40 and 0.49 μs.[25, 31, 32]

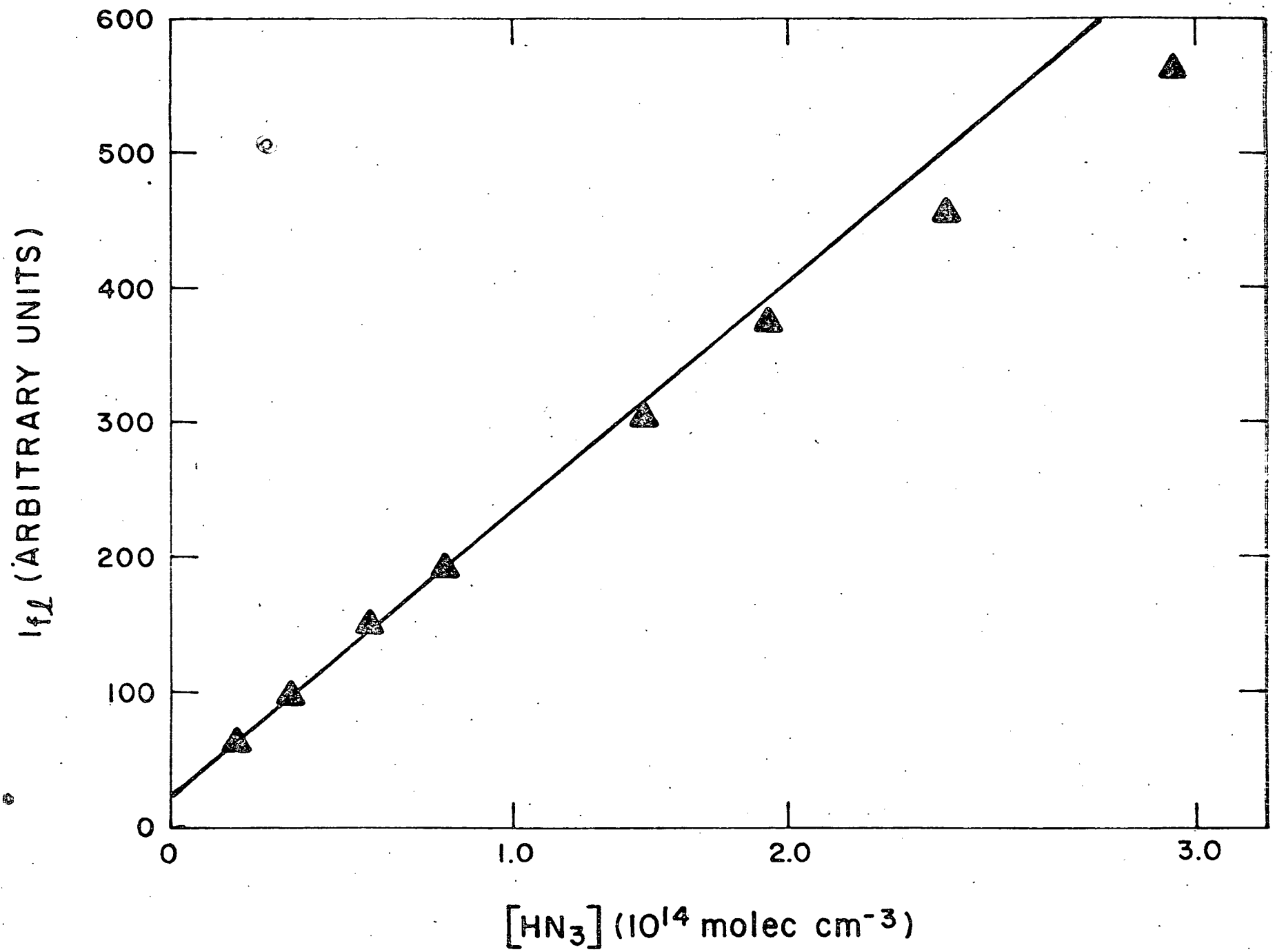

Fig. 4 LIF Intensity, Proportional to $[NH(a^1\Delta)]$, as a Function of $[HN_3]$ for a Photolysis-Laser Energy of ~ 125 μJ and a Delay Time of ~ 2 μs

For fixed $[HN_3]$, the $NH(a\,^1\Delta)$ LIF intensity shows a first-order decay as the time between the photolysis and probe lasers is increased, Fig. 5. This is most likely the result of removal of the $NH(a\,^1\Delta)$ by HN_3, reaction 2. After termination of the photolysis-laser pulse, the rate equation for the concentration of $[NH(a\,^1\Delta)]$ with time is

$$\frac{d[NH(a\,^1\Delta)]}{dt} = - k_2 [NH(a\,^1\Delta)] [HN_3] \quad . \tag{21}$$

Under pseudo first-order conditions($[HN_3] \gg [NH(a\,^1\Delta)]$), this equation is easily solved, and

$$\ln \frac{[NH(a\,^1\Delta)]}{[NH(a\,^1\Delta)]_o} = - k_2 [HN_3] t \quad . \tag{22}$$

Thus, semi-log plots of the concentration of $NH(a\,^1\Delta)$ (or the LIF intensity which is directly proportional to that concentration) versus time will be linear with slopes equal to $-k_2[HN_3]$. Such linear plots are shown in Fig. 5. If several decay slopes are measured at varying values of $[HN_3]$, then a plot of the inverse of the decay slopes versus $[HN_3]$ will give a straight line whose slope will be equal to k_2. Such a plot is shown in Fig. 6. The rate constant, k_3, for the removal of $NH(a\,^1\Delta)$ by HN_3 obtained from Fig. 6 is 1.7×10^{-10} cm^3 $molec^{-1}$ s^{-1}. This is about a factor of two larger than previously reported values,[2,5] but is a more direct determination than these previous measurements, and, furthermore, agrees with a detailed analysis of $NH_2(\tilde{A}\,^2A_1)$ fluorescence traces given below.

The finite intercept in Fig. 6 probably results from the quenching of $NH(a\,^1\Delta)$ by the argon bath gas. The rate constant for that process is obtained by dividing the intercept in Fig. 6 by the argon number density. The resultant rate constant is 1.2×10^{-14} cm^3 $molec^{-1}$ s^{-1}. This number will be checked in further experiments in which the argon pressure is varied.

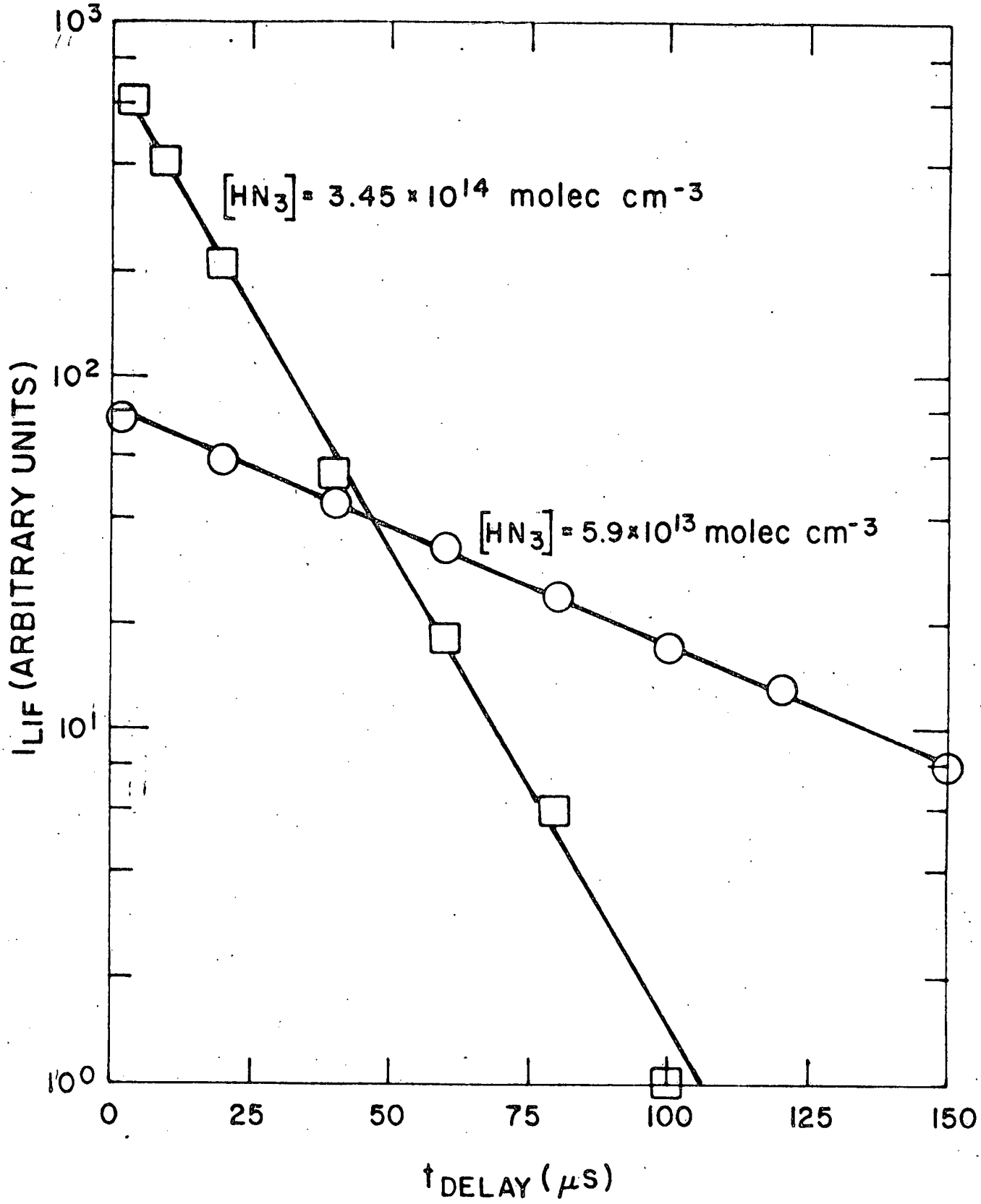

Fig. 5 Decay of NH($a^1\Delta$) LIF Intensity as a Function of Delay Time Between Photolysis and Probe Lasers

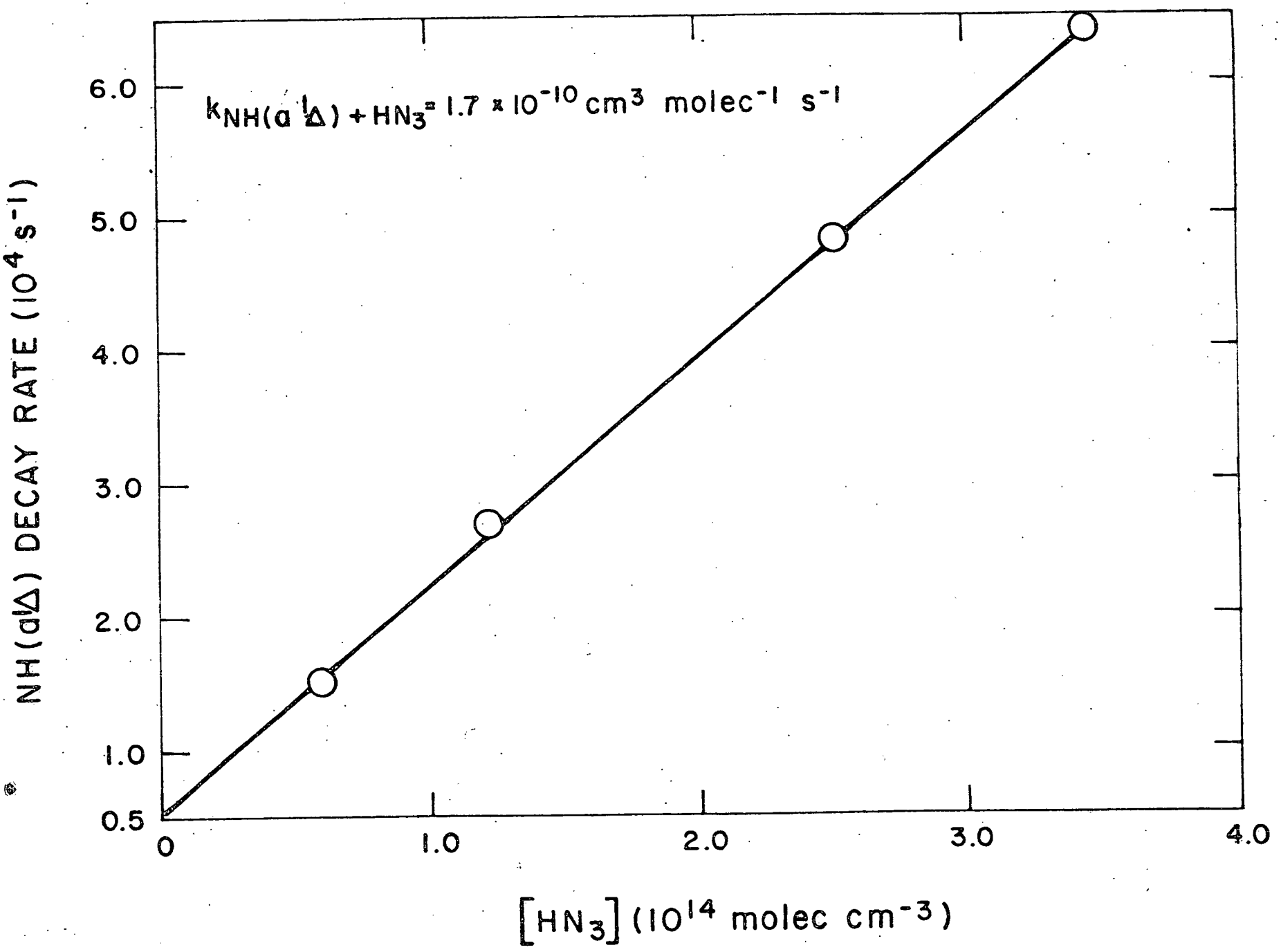

Fig. 6 Rate of Decay of NH($a^1\Delta$) as a Function [HN_3]. (P_{Ar} = 15 torr).

The fluorescence observed when low pressures of pure HN_3 are photolyzed is due to emission from the $NH_2(\tilde{A}\ ^2A_1) \rightarrow NH_2(\tilde{X}\ ^2B_1)$ system, the so-called α-bands of ammonia, extending from about 450 nm to 900 nm[7]. Typical oscilloscope-traces of this fluorescence are shown in Fig. 7. The fluorescence traces were fit via a least squares program to a kinetic model incorporating reactions 2-4. The rate equation for the concentration of $NH_2(\tilde{A}\ ^2A_1)$ is

$$\frac{d[NH_2(\tilde{A}\ ^2A_1)]}{dt} = k_2\,[NH(a\ ^1\Delta)]\,[HN_3] - (k_3 + k_4\,[HN_3])\,[NH_2(\tilde{A}\ ^2A_1)] \quad (23)$$

By assuming that the $NH(a\ ^1\Delta)$ is formed instantaneously, Eq. 22 may be inserted into Eq. 23 for the concentration of $NH(a\ ^1\Delta)$ and the resulting expression is solveable analytically, viz.

$$[NH_2(\tilde{A}\ ^2A_1)] = \frac{k_2[HN_3]\,[NH(a\ ^1\Delta)]_o}{k_3 + k_4[HN_3] - k_2[HN_3]} \left\{ e^{-k_2[HN_3]t} - e^{-(k_3 + k_4[HN_3])t} \right\} \quad (24)$$

The $NH(a\ ^1\Delta)$ is formed in the photolysis laser pulse with a FWHM of about 0.6 μs. Thus the assumption used to solve Eq. 23 will be reasonably good for HN_3 pressures below 120 mtorr for which the $NH_2(^2A_1)$ fluorescence extends over 15 μs.

The intensity of the fluorescence from $NH_2(\tilde{A}^2A_1)$ is just k_3 (the radiative-decay rate constant) times the concentration of that species. The concentration of $NH(a\ ^1\Delta)$ at t = 0 is given by

$$[NH(a^1\Delta)]_o = \kappa\, I_{laser}\,[HN_3] \quad , \quad (25)$$

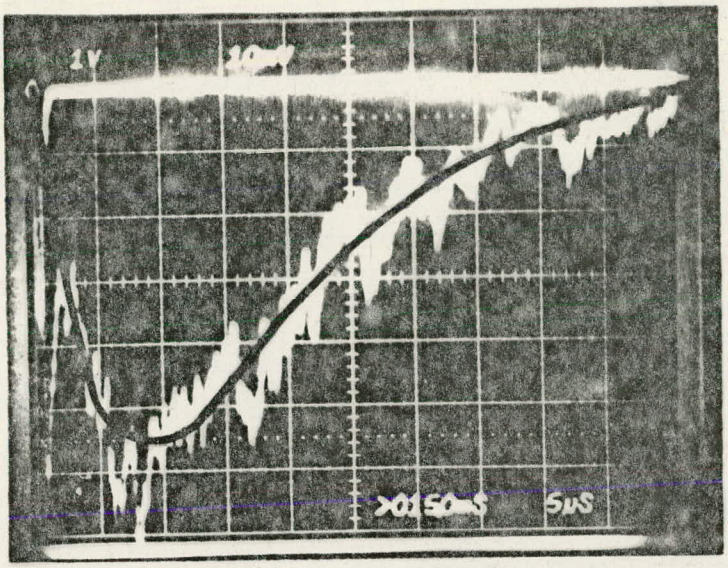

P = 18 mtorr

R_L = 3.42 kΩ

Vertical: 10 mV/cm

Horizontal: 5 μs/cm

10 mV = 13.2 photoelectrons/μs

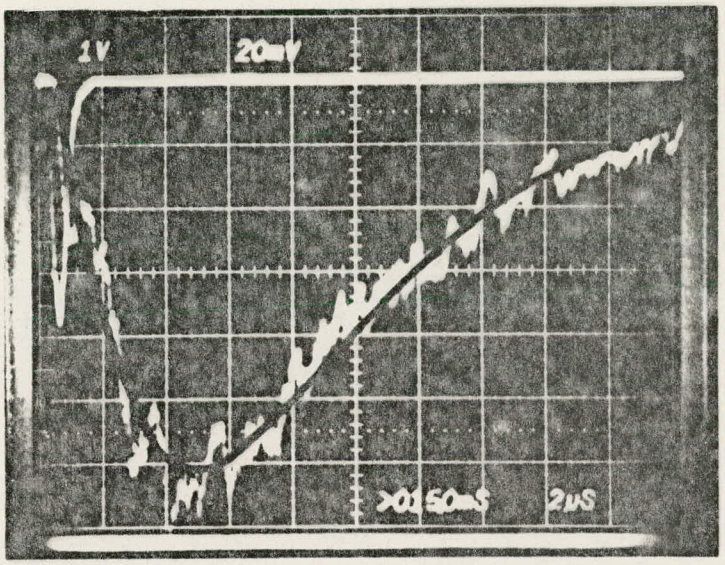

P = 49.5 mtorr

R_L = 1.9 kΩ

Vertical: 20 mV/cm

Horizontal: 2 μs/cm

10 mV = 23.8 photoelectrons/μs

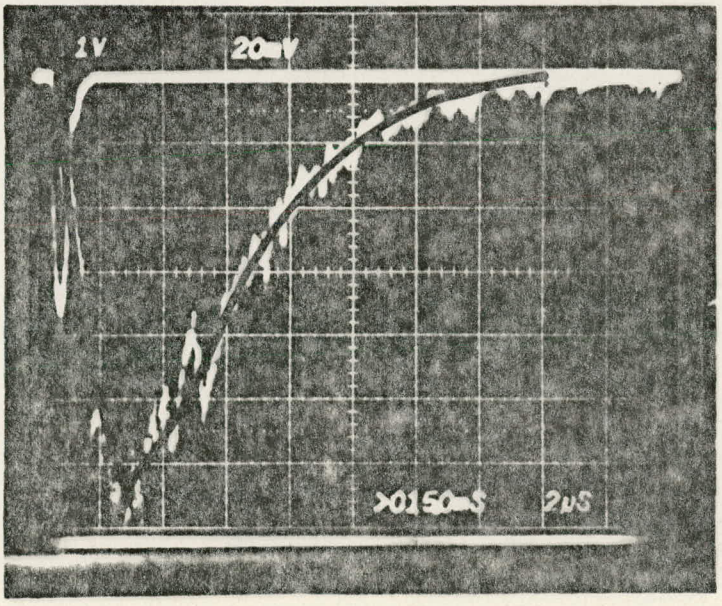

P = 112 mtorr

R_L = 0.75 kΩ

Vertical: 20 mV/cm

Horizontal: 2 μs/cm

10 mV = 60.3 photoelectrons/μs

Fig. 7 NH_2 ($\tilde{A}\,^2A_1$) Fluorescence following Photolysis of HN_3 at 296 nm. The spike at early time is the photolysis-laser pulse, the energy of which is ~ 650 μJ for all three traces. The solid lines through the fluorescence traces are the least-squares fits of Eq. (26) to the data.

where I_{laser} is the intensity of the photolysis laser and κ is a constant which includes such things as laser-beam cross-sectional area, absorption coefficient of HN_3 at the photolysis wavelength, and diameter of the viewing region. Thus, the intensity of the NH_2 emission as a function of time is given by

$$I_{fl} = \frac{\zeta k_3 k_2 [HN_3]^2 I_{laser}}{k_3 + k_4[HN_3] - k_2[HN_3]} \left\{ e^{-k_2[HN_3]t} - e^{-(k_3 + k_4[HN_3])t} \right\} \qquad (26)$$

where ζ is a constant which incorporates κ plus other experimental quantities such as photomultiplier quantum efficiency, the fraction of total emission occurring within the pass band of the detection system, and optical-system collection efficiency. A number of fluorescence traces taken at pressures between 18 and 112 mtorr were fit simulaneously to expression 26 using a non-linear least squares routine to determine the parameters k_2, k_3, k_4, and ζ. The computer-fit rate constants are, $k_2 = 1.5 \times 10^{-10}$ cm^3 molec^{-1} s^{-1}, $k_3 = 9.75 \times 10^4$ s^{-1}, and $k_4 = 8.0 \times 10^{-11}$ cm^3 molec^{-1} s^{-1}. The value obtained for k_2 is in good agreement with the value obtained from the direct measurement of the decay of $NH(a^1\Delta)$. The deduced value for k_3 yields a fluorescence lifetime for $NH_2(\tilde{A}^2A_1)$ of 10.3 μs, in agreement with the results of Halpern et al.[19] who measured values between about 7 and 25 μs for various vibronic levels of the $NH_2(\tilde{A}^2A_1)$ state by measuring directly the fluorescence decay of the excited NH_2 following excitation with a tuneable dye laser. Some typical fits of the NH_2 fluorescence traces are shown in Fig. 7 by the solid lines.

The ratio of k_4/k_3 may be determined directly from the data without resorting to computer fitting. Integrating Eq. 26 over time gives

$$I_{fl} = \frac{\zeta k_3 [HN_3] I_{laser}}{k_3 + k_4[HN_3]} \qquad (27)$$

This expression may be rearranged and inverted to give

$$\frac{I_{laser}}{I_{fl}} = \frac{k_4}{\zeta k_3} + \frac{1}{\zeta[HN_3]} \qquad (28)$$

Thus, a plot of the ratio of photolysis energy to the total fluorescence intensity versus the reciprocal of the HN_3 pressure should be linear, and the resulting ratio of the intercept to slope will be the ratio k_4/k_3. The data are plotted in this fashion in Fig. 8, and yield a ratio of 25.3 $torr^{-1}$ which is in good agreement with the ratio k_4 to k_3 of 23.6 $torr^{-1}$ obtained from the computer fit to the fluorescence traces.

C. Photolysis of ClN_3

A few preliminary experiments were performed on the photolysis of chlorine azide. This molecule has never been photolyzed previously, although a few experiments have been reported on the thermal decomposition[8] and the reactivity of ClN_3 with several atoms.[33-35] For photolysis experiments requiring small amounts of ClN_3, the compound is easily generated by slowly flowing highly dilute mixtures of Cl_2 in argon through a column packed with sodium azide. About half the Cl_2 is converted to ClN_3 by this technique. Higher Cl_2 conversion efficiencies are possible if ~ 1% water is added to the reaction mixture, but then HN_3 contamination results.[33]

Photolysis of ClN_3 at 300 nm resulted in prompt emission in the red. The CG 2-62 filter/9659QA PMT combination was used in these studies (600 nm ≤ λ ≤ 900 nm). This emission arises from the $NCl(b^1\Sigma^+ - X^3\Sigma^-)$ system for which λ_{oo} = 665 nm.[10] Most of the ClN_3 decomposed with the first pulse, as subsequent pulses resulted in greatly reduced light emission (see Fig. 9). This is in spite of the fact that the total volume of the photolysis cell is on the order of 11 liters, while the volume of gas illuminated by the photolysis laser was about 40 ml. The time between laser pulses was

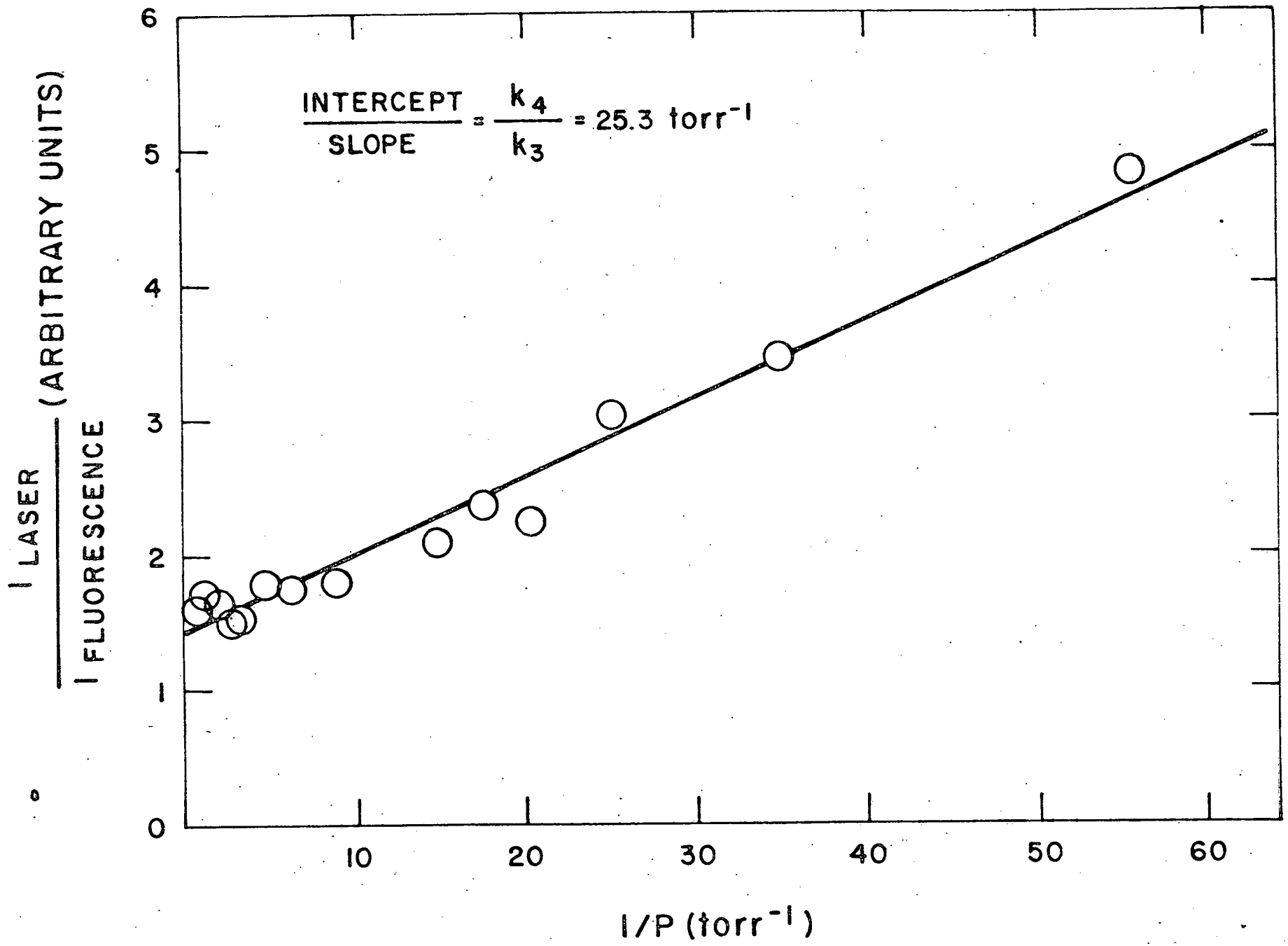

Fig. 8 Ratio of Photolysis-Laser Energy to Total $NH_2(^2A_1)$ Fluorescence Yield in the Photolysis of HN_3 as a Function of Reciprocal Pressure

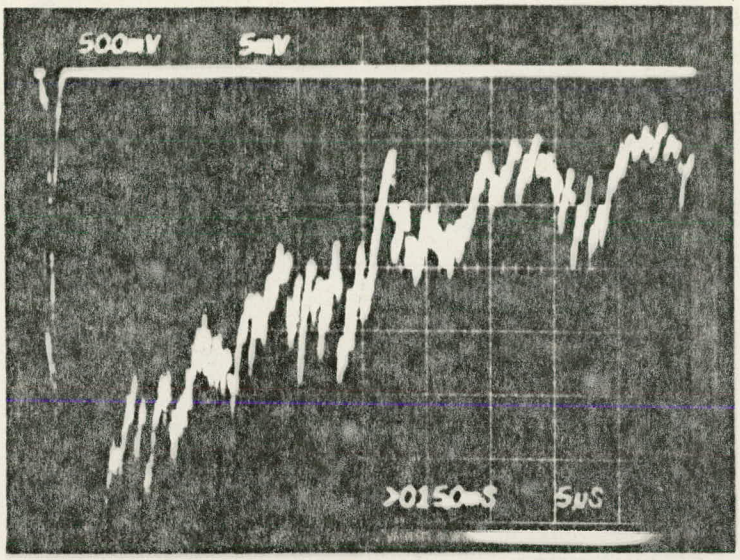

P_{total} = 1.1 torr
shot #1
R_L = 5.65 kΩ

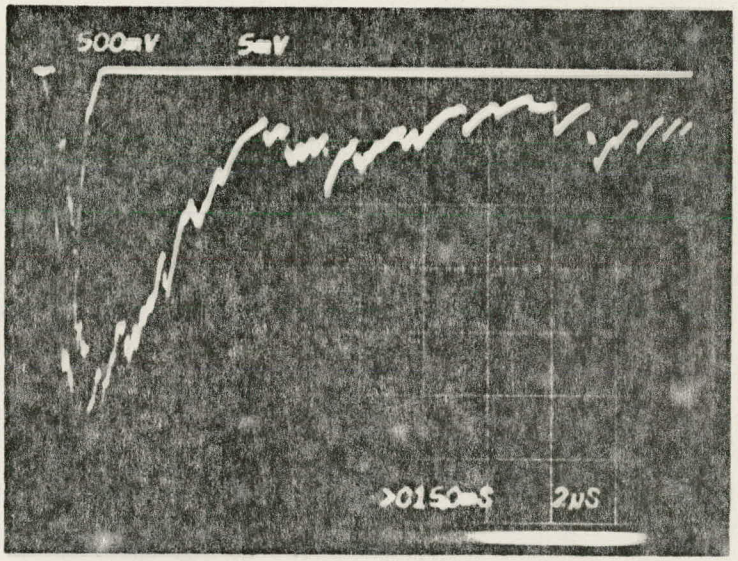

P_{total} = 1.1 torr
shot #2
R_L = 5.65 kΩ

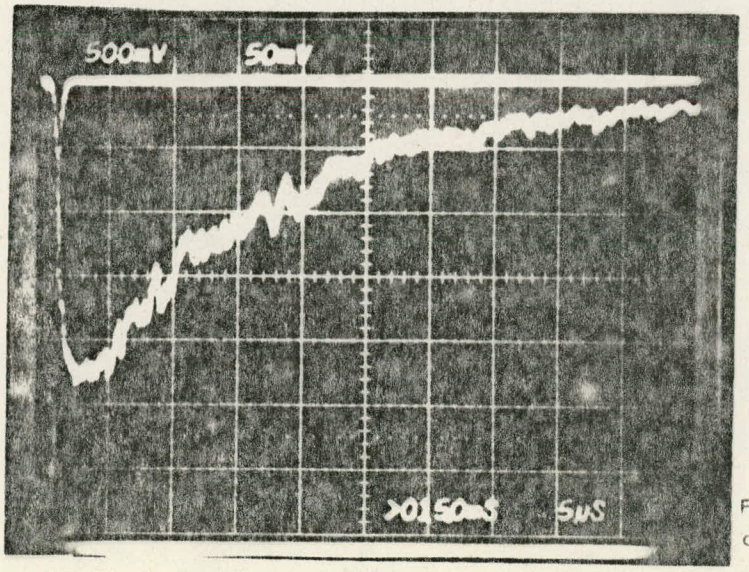

P_{total} = 5.2 torr
shot #1
R_L = 2.62 kΩ

Fig. 9 NCl ($b^1\Sigma^+$) Fluorescence following Photolysis of ClN_3 at 300 nm.

sufficiently long that diffusion of gas back into the observation region should have been complete. At higher argon bath-gas pressures, the rapid decay of ClN_3 was moderated somewhat, but still significant decomposition was evident after only a few shots (Fig. 10). Thus, the photolysis pulse appears to initiate a rapid chemical decomposition of ClN_3 via a chain mechanism. These observations indicate the extreme instability of ClN_3. By contrast, HN_3 is much more stable since repeated photolysis of pure HN_3 at pressures up to 2 torr results in no noticeable degredation in the light emission from $NH_2(^2A_1)$. The maximum ClN_3 partial pressure studied was only ~ 200 mtorr.

The rate of decay of the ClN_3 was studied as a function of pressure of the $ClN_3/Cl_2/Ar$ mixture. Several decay plots are shown in Fig. 11. A kinetic analysis of the emission similar to that given above for the disappearance of $NH(a^1\Delta)$ indicates that the fluorescence decay should be exponential, and that furthermore, the rate constant for quenching processes can be determined from the slope of a plot of the decay rates versus pressure (analogous to Fig. 5 for NH). To date, we have not been able to study the kinetics of the fluorescence decay in detail, so we are not able to say whether the observed quenching is by argon, unreacted Cl_2, or undissociated ClN_3. Figure 12 shows the quenching plot, where the pressure plotted is the pressure of the argon bath gas. If the fluorescence is quenched by the argon, the rate constant would be 1.6×10^{-13} cm^3 molec^{-1} s^{-1}, a value which seems large in view of the fact that electronically excited diatomic molecules are usually quenched by argon with rate constants of about 10^{-15} to 10^{-17} cm^3 molec^{-1} s^{-1}. If the quenching were either by unreacted Cl_2 or ClN_3, the quenching rate constant would be 1.6×10^{-11} cm^3 molec^{-1} s^{-1} assuming a 50% yield for conversion of Cl_2 to ClN_3. This point will be checked in future experiments.

The intercept from Fig. 12 is 3.47×10^4 s^{-1}. In principle, this value should correspond to the fluorescence lifetime to $ClN(b^1\Sigma^+)$. If such were the case, the lifetime of this state would be 28.8 μs. However, we expect a much longer lifetime for this state, since the transition to the ground state is highly forbidden. Future experiments will be performed to answer this question.

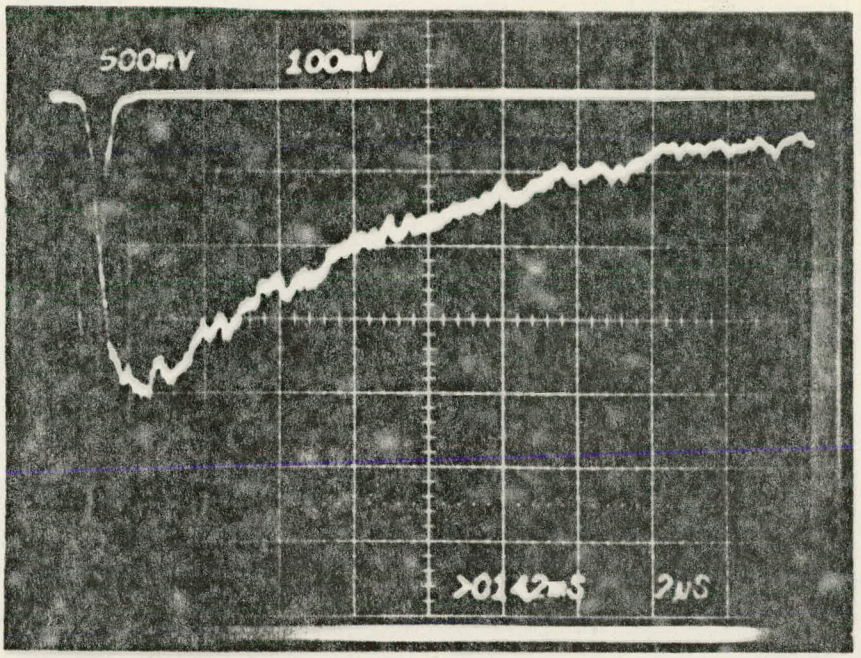

P_{total} = 15.2 torr

Shot #1

R_L = 1.1 kΩ

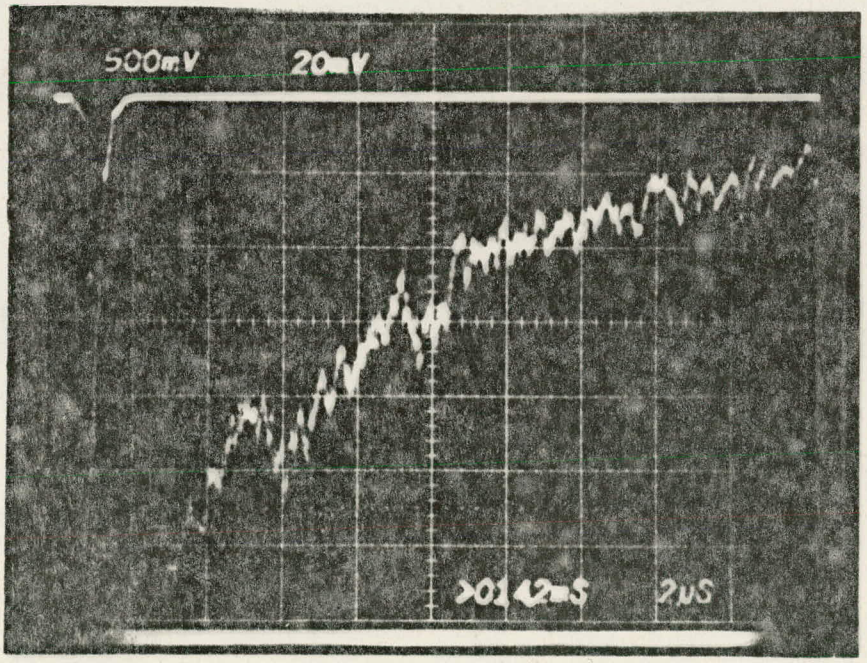

P_{total} = 15.2 torr

After ~ 30 shots

R_L = 1.1 kΩ

Fig. 10 NCl ($b\,^1\Sigma^+$) Fluorescence following Photolysis of ClN_3 at 300 nm.

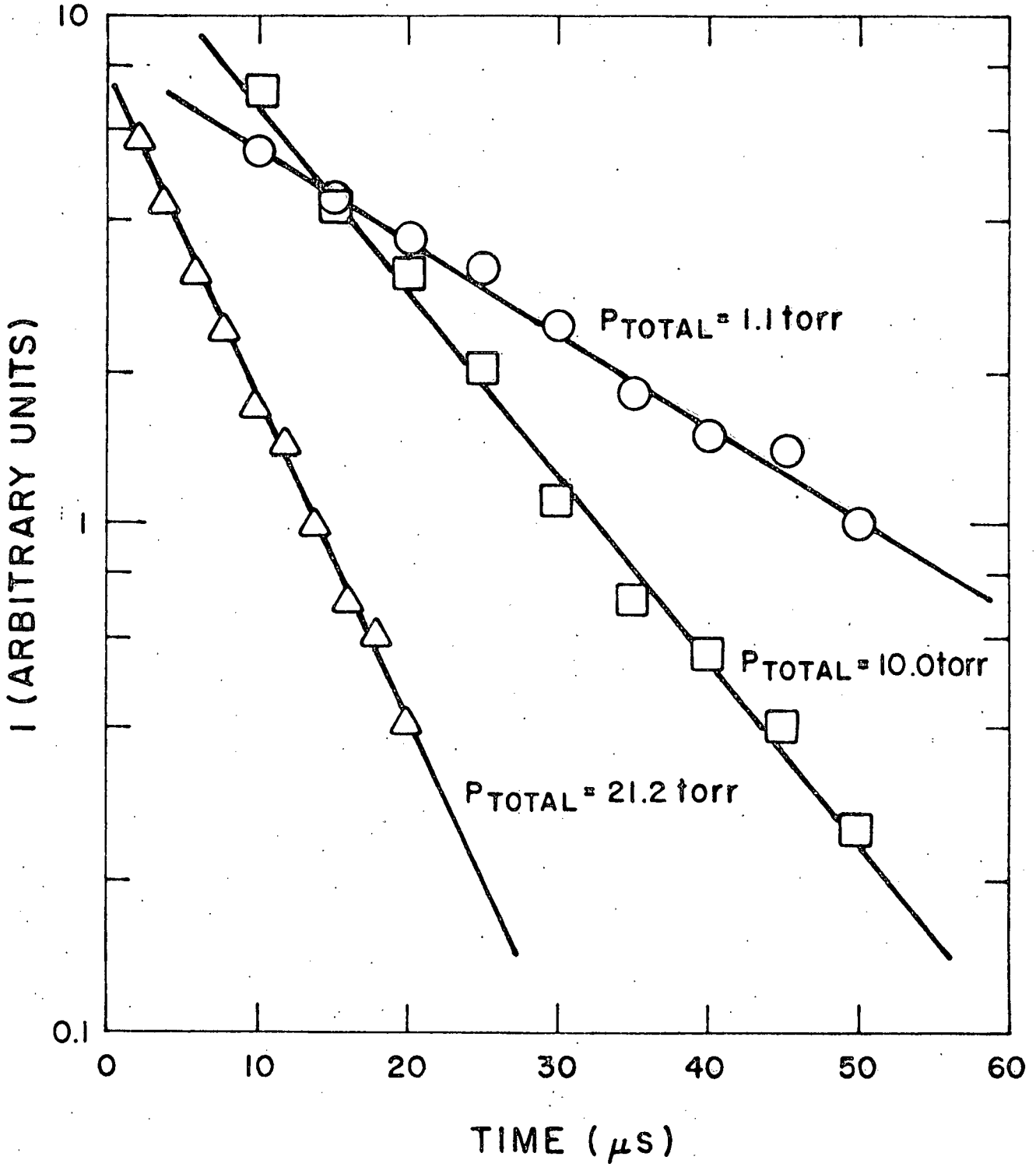

Fig. 11 $NCl(b^1\Sigma^+)$ Fluorescence Decay at Several Different Pressures Following the Photolysis of ClN_3 at 300 nm. ($X_{ClN_3} \sim 0.01$, $X_{Cl_2} \sim 0.01$, $X_{Ar} = 0.98$).

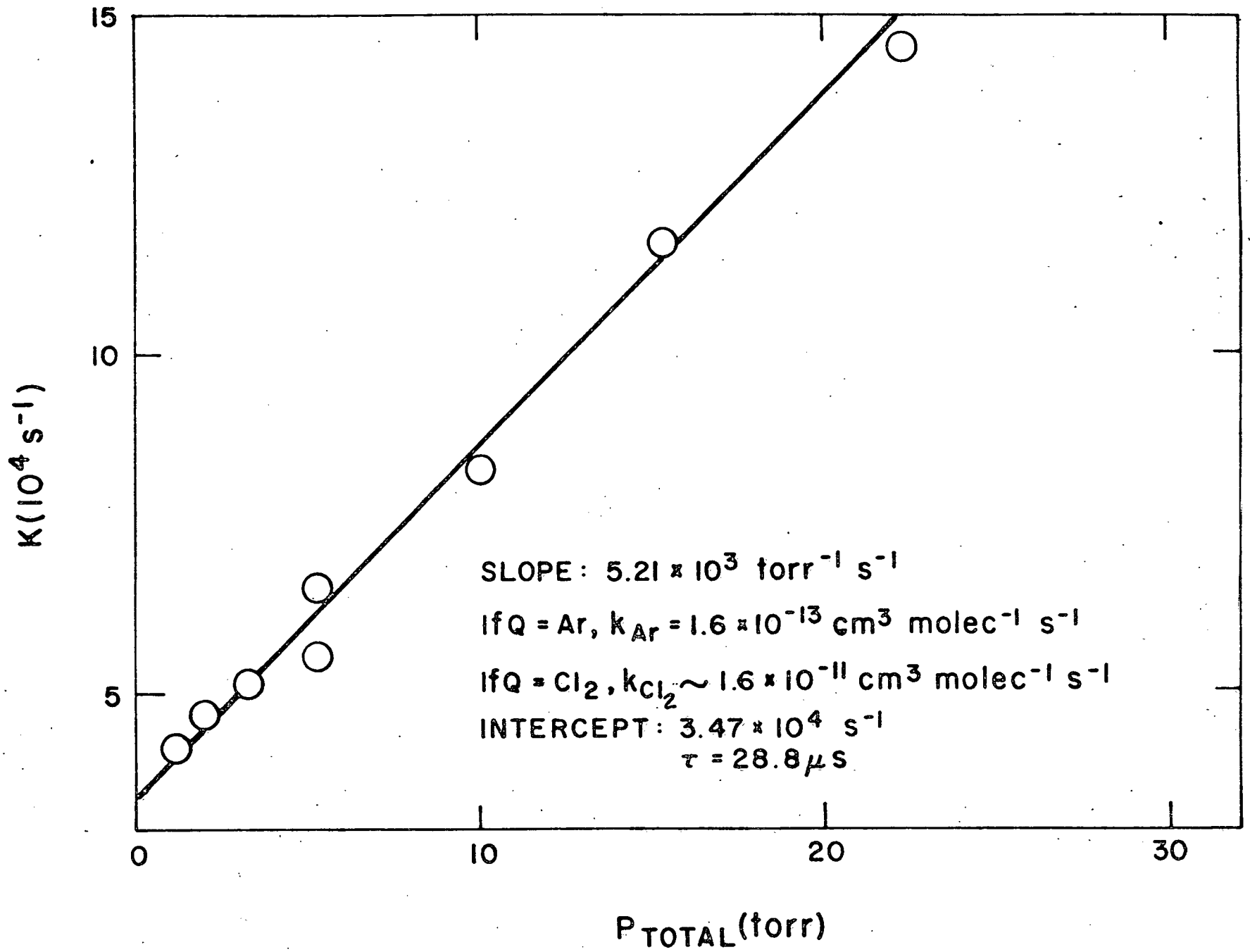

Fig. 12 $NCl(b^1\Sigma^+)$ Fluorescence Decay Rates as a Function of Total Pressure from ClN_3 Photolysis at 300 nm. ($X_{ClN_3} \sim 0.01$, $X_{Cl_2} \sim 0.01$, $X_{Ar} = 0.98$).

IV. SUMMARY

A photochemical reactor was designed and built to study the wavelength-selected photolysis of gaseous azides. The apparatus incorporates a frequency-doubled, tuneable dye laser as the photolysis source, and has a second tuneable dye laser which may be used to probe the density of photolysis fragments by laser-induced fluorescence. Some tests on the LIF detection of OH indicate a sensitivity on the order of 10^8 molec cm^{-3} in agreement with design. Experiments on the photolysis of HN_3 have shown that the initial product produced in the photolysis is $NH(a^1\Delta)$ and N_2, and that furthermore the $NH(a^1\Delta)$ reacts with HN_3 to produce $NH_2(\tilde{A}^2A_1)$. Observations on the time dependence of $NH(a^1\Delta)$ number density (probed by LIF) and the intensity of the $NH_2(\tilde{A}^2A_1)$ fluorescence have been analyzed to give rate constants for the removal of $NH(a^1\Delta)$ and $NH_2(\tilde{A}^2A_1)$ by HN_3. Preliminary experiments were performed on the photolysis of ClN_3, which showed that the photolysis resulted in prompt emission from $NCl(b^1\Sigma^+)$ between 600 and 800 nm. Further experiments are in progress to determine the lifetime of this potential laser species as well as its reactivity with respect to other molecules.

REFERENCES

1. L. G. Piper and R. L. Taylor, "Investigation of Induced Unimolecular Decomposition for Development of Visible Chemical Lasers", PSI TR-96 under ERDA contract No. EY-76-C-02-2920. *000 (1977).

2. J. R. McDonald, R. G. Miller and A. P. Baronavski, Chem. Phys. Lett. 51, 57 (1977).

3. B. A. Thrush, Proc. Roy. Soc. A235, 143 (1956).

4. F. Stuhl, dissertation, the University of Bonn, Bonn, Germany (1966).

5. R. J. Paur and E. J. Bair, Int. J. Chem. Kinet. 8, 139 (1976).

6. P. I. Stepanov, et.al., Vestn. Mosk. Univ. Khim. 14(3), 306 (1973).

7. R. W. Pearse and A. G. Gaydon, The Identification of Molecular Spectra, 4th ed. London: Chapman and Hall, 234 (1976).

8. K. Gleu, Z. Phys. 38, 176 (1926).

9. G. Pannetier and A. G. Gaydon, J. Chim. Phys. 48, 221 (1951).

10. R. Colin and W. E. Jones, Can. J. Phys. 45, 301 (1967).

11. J. M. Herbelin, D. J. Spencer and M. A. Kwok, J. Appl. Phys. 48, 3050 (1977).

12. B. Gelernt, S. V. Filseth and T. Carrington, Chem. Phys. Lett. 36, 238 (1975).

13. J. M. Herbelin, Chem. Phys. Lett. 42, 367 (1976).

14. C. Zetzsch and F. Stuhl, Chem. Phys. Lett. 33, 375 (1975).

15. C. Zetzsch and F. Stuhl, Ber. Bunsenges. Physik. Chem. 80, 1348 (1976).

16. C. Zetzsch and F. Stuhl, J. Chem. Phys. 66, 3107 (1977).

17. B. Gelernt, S. V. Filseth and T. Carrington, J. Chem. Phys., 65, 4940 (1976).

18. L. G. Piper and R. L. Taylor, "Investigation of Concept of Efficient Short-Wavelength Laser", PSI TR-120 under ERDA contract No. EC-77-C-02-4223 (1978).

19. J. B. Halpern, G. Hancock, M. Lenzi and K. H. Welge, J. Chem. Phys. 63, 4808 (1975).

20. J. R. McDonald, J. W. Rabalais and S. P. McGlynn, J. Chem. Phys. 52, 1332 (1970).

21. A. C. G. Mitchell and M. W. Zemansky, Resonance Radiation and Excited Atoms, Cambridge: The University Press, (1971).

22. L. G. Piper and R. L. Taylor, "Investigation of Concept of Efficient Short Wavelength Laser", PSI TR-98 Under ERDA Contract No. EC-77-C-02-4223 (1977).

23. Private communication from Jan Archambault (Princeton Applied Research Corporation)(1977).

24. RCA Photomultiplier Manual, Harrison, NJ: RCA Corporation, 56-76 (1970).

25. W. H. Smith, J. Brzozowski and P. Erman, J. Chem. Phys. 64, 4628 (1976).

26a. J. Crank, The Mathematics of Diffusion, Oxford: The Clarendon Press, 26-28 124 (1957).

26b. We thank Dr. N. H. Kemp of PSI for studying the diffusion problem.

27. J. A. Silver, W. L. Dimpfl, J. H. Brophy and J. L. Kinsey, J. Chem. Phys. 65, 1811 (1976).

28. K. R. German, J. Chem. Phys. 62, 2584 (1975).

29. W. L. Dimpfl, private communication (1978).

30. H. Gerzberg, Molecular Spectra and Molecular Structure I. The Spectra of Diatomic Molecules, New York: Van Nostrand Reinhold Company, 46 (1950).

31. W. H. Smith, J. Chem. Phys. 51, 520 (1969).

32. E. Fink and K. H. Welge, Z. Naturf. 19a 1193 (1964).

33. T. C. Clark and M. A. A. Clyne, Trans. Faraday Soc. 65, 2994 (1969).

34. T. C. Clark and M. A. A. Clyne, Trans. Faraday Soc. 66, 877 (1970).

35. J. Combourieu, G. LeBras, G. Poulet and J. L. Jourdain, XVI Int. Comb. Symp. 863, (1976).

REPORT DISTRIBUTION LIST

for Contract No. ES-77-C-02-4223.A002

Dr. Paul Hoff (6 copies)
New Laser Programs Manager
Office of the Assistant Director
for Laser Fusion
Office of Laser Fusion, C-404
Department of Energy
Washington, D.C. 20545

Dr. John Emmett
Associate Director for Lasers
University of California
Lawrence Livermore Laboratory
Post Office Box 808
Livermore, CA 94550

Dr. O'Dean Judd
University of California
Los Alamos Scientific Laboratory
Post Office Box 1663
Los Alamos, New Mexico 87545

Dr. James Gerardo
Sandia Laboratories
Post Office Box 5800
Albuquerque, New Mexico 87115

Dr. Donald Setser
Kansas State University
Department of Chemistry
Manhatten, Kansas 66506

Dr. Walter Stevens
Physical Chemistry Division
National Bureau of Standards
Washington, D.C. 20234

Dr. Morris Krauss
Physical Chemistry Division
National Bureau of Standards
Washington, D.C. 20234

Mr. Harold N. Miller, Director (2 copies)
Contracts Management Office
Department of Energy
9800 South Cass Avenue
Argonne, Illinois 60439

Dr. George Sanzone
Virginia Polytechnic Institute
Department of Chemistry
Blacksburg, Virginia 24061

Dr. Robert Center
Mathematical Sciences Northwest, Inc.
Post Office Box 1887
Bellevue, Washington 98009

Dr. Gerald L. Rogoff
Westinghouse Electric Corporation
1310 Beulah Road
Pittsburgh, Pennsylvania 15235

Dr. William F. Krupke
Lawrence Livermore Laboratory
L-258
Post Office Box 808
Livermore, California 94550

Professor M. S. Lubell
Yale University
New Haven, Connecticut 06520

Dr. Charles K. Rhodes
University of Illinois
Illinois

Dr. Thomas A. Barr, Jr.
DRCPM-HEL-R
Building 8978
Redstone Arsenal, Alabama 35809

REPORT DISTRIBUTION LIST (cont'd)

Prof. Shaul Yatsiv
Racah Institute of Physics
Hebrew University
Jerusalem, Israel

Dr. Joseph Mangano
Defense Advanced Research
Project Agency
Strategic Technical Office
1400 Wilson Boulevard
Arlington, VA 22209

Dr. Charles von Rosenberg
Avco Everett Research Lab., Inc.
2385 Revere Beach Parkway
Everett, MA 02149

Dr. J. Doyle McClure
Boeing Company
P. O. Box 3999
Seattle, Washington 98124